Inorg. Chem. **2005**, *44*, 9852–9861

Tetra-2,3-pyrazinoporphyrazines with Externally Appended Pyridine Rings. 3. A New Highly Electron-Deficient Octacationic Macrocycle: Tetrakis-2,3-[5,6-di{2-(*N*-methyl)pyridiniumyl}pyrazino]porphyrazine, $[(2\text{-Mepy})_8\text{TPyzPzH}_2]^{8+}$

Costanza Bergami,[§] Maria Pia Donzello,[§] Claudio Ercolani,*[,§] Fabrizio Monacelli,*[,§] Karl M. Kadish,*[,||] and Corrado Rizzoli[#]

Dipartimento di Chimica, Università degli Studi di Roma "La Sapienza", p.le A. Moro 5, I-00185 Roma, Italy, Department of Chemistry, University of Houston, Houston, Texas 77204-5003, and Dipartimento di Chimica Generale ed Inorganica, Università di Parma, Viale delle Scienze, I-43100 Parma, Italy

Received June 30, 2005

A new octacationic macrocycle, tetrakis-2,3-[5,6-di{2-(*N*-methyl)pyridiniumyl}pyrazino]porphyrazine, was obtained in its hydrated form as the water-soluble iodide salt. This compound, abbreviated as $[(2\text{-Mepy})_8\text{TPyzPzH}_2](I_8)\cdot 8H_2O$ (2-Mepy = 2(*N*-methyl)pyridiniumyl moiety), was obtained by demetalation of the corresponding Mg^{II} complex, $[(2\text{-Mepy})_8\text{TPyzPzMg}(H_2O)](I_8)\cdot 5H_2O$, which in turn was prepared from its corresponding neutral hydrated species tetrakis-2,3-[5,6-di(2-pyridyl)pyrazino]porphyrazinato(monoaquo)magnesium(II), $[\text{Py}_8\text{TPyzPzMg}(H_2O)]\cdot 4H_2O$, by reaction with CH_3I in *N*,*N*-dimethylformamide. The quaternization reactions by using CH_3I or methyl *p*-toluenesulfonate were also conducted on the monomeric precursor 2,3-dicyano-5,6-di(2-pyridyl)-1,4-pyrazine, $[(CN)_2\text{Py}_2\text{Pyz}]$, with formation of the monoquaternized ion $[(CN)_2\text{Py}(2\text{-Mepy})\text{Pyz}]^+$ neutralized by iodide and *p*-toluenesulfonate anions. Single-crystal X-ray work allowed elucidation of the structure of the two salt-like species. The diquaternized ion $[(CN)_2(2\text{-Mepy})_2\text{Pyz}]^{2+}$ could also be obtained as a *p*-toluenesulfonate salt, but attempts at direct macrocyclization of this dicationic species were unsuccessful. The iodide salt $[(2\text{-Mepy})_8\text{TPyzPzH}_2](I_8)\cdot 8H_2O$ is water-soluble, with different solubilities depending on the range of pH explored. It was established that the macrocycle $[(2\text{-Mepy})_8\text{TPyzPzH}_2]^{8+}$ undergoes facile deprotonation and behaves as a strong acid. Aggregation phenomena are observed for both the octacation $[(2\text{-Mepy})_8\text{TPyzPzH}_2]^{8+}$ and its corresponding centrally deprotonated species $[(2\text{-Mepy})_8\text{TPyzPz}]^{6+}$. Nevertheless, both cationic moieties exist in their monomeric form under specific experimental conditions. UV–visible monitored titrations with NaOH provide information about the type of protonation/deprotonation equilibria which are complicated by the occurrence of aggregation phenomena.

Introduction

Recent reviews on water-soluble porphyrins[1] provide a picture of the enormous amount of material published on this topic in terms of structure and uses of naturally occurring and synthetic mono- or multiply charged porphyrins. Water-soluble tetraazaporphyrins, i.e., phthalocyanines or other different, mainly cationic porphyrazines such as those derived from pyridino- or pyrazinoporphyrazines,[2,3] have also been prepared and investigated, although they have been relatively much less extensively studied.

* To whom correspondence should be addressed. E-mail: claudio.ercolani@uniroma1.it (C.E.), kkadish@uh.edu (K.M.K.), fabrizio.monacelli@uniroma1.it (F.M.).
§ Università degli Studi di Roma "La Sapienza".
|| University of Houston.
Università di Parma.

(1) (a) Hambright, H. Chemistry of Water Soluble Porphyrins. In *The Porphyrin Handbook*; Kadish, K. M., Smith, K. M., Guilard, R., Eds.; Academic Press: New York, 2000; Vol. 3, Chapter 18, pp 129−210. (b) Koji, K. *J. Porphyrins Phthalocyanines* **2004**, *8*, 148. (c) Makarska, M.; Radzki, S. *Ann. Univ. Mariae-Sklodowska, Sect. AA: Chem.* **2002**, *57*, 332−363.

(2) (a) Leznoff, C. C. In *Phthalocyanines − Properties and Applications*; Leznoff, C. C., Lever, A. B. P., Eds.; VCH Publishers: New York, 1993; Vol. 1, pp 2−54. (b) Kudrevich, S. V.; van Lier, J. E. *Coord. Chem. Rev.* **1996**, *156*, 163−182.

(3) Stuzhin, P. A.; Ercolani, C. *The Porphyrin Handbook*; Kadish, K. M., Smith, K. M., Guilard, R., Eds.; Academic Press: New York, 2003; Vol. 15, Chapter 101, pp 263−364.

10.1021/ic051084l CCC: $30.25
Published on Web 11/19/2005

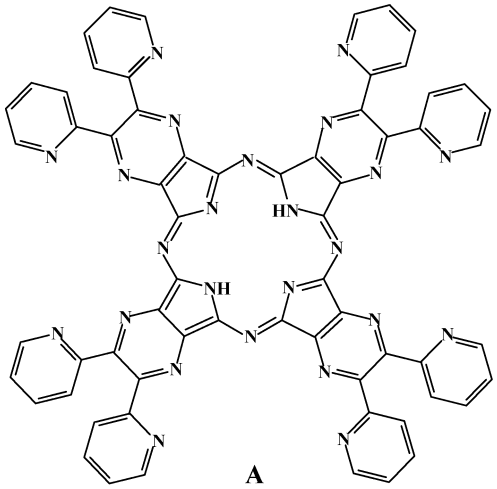

A

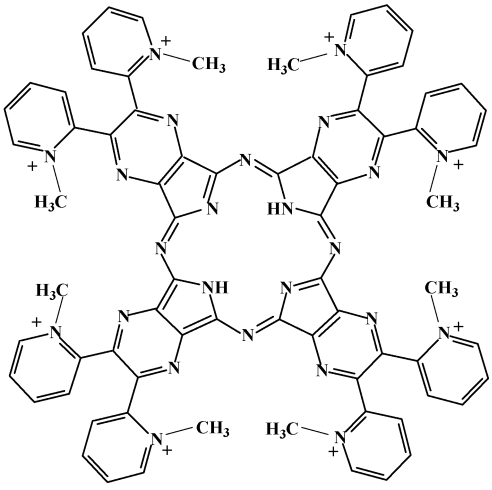

B

Figure 1. Schematic representations of (A) $[Py_8TPyzPzH_2]$ and (B) $[(2\text{-Mepy})_8TPyzPzH_2]^{8+}$.

Following our studies on the synthesis and characterization of new porphyrazine macrocycles carrying heterocyclic rings annulated to the pyrrole rings of the internal tetrapyrrolic core,[4] we have recently reported on a novel tetrapyrazinoporphyrazine macrocycle carrying eight externally appended pyridine rings, i.e., tetrakis-2,3-[5,6-di(2-pyridyl)pyrazino]-porphyrazine (Figure 1A), $[Py_8TPyzPzH_2]$,[5a] and a number of its metal derivatives.[5b]

The main feature shared by this novel class of macrocycles and the other porphyrazine analogues[4,5] is the intrinsically electron-deficient character generated by the presence of the peripheral annulated five-, six-, or seven-membered heterocyclic rings containing N, S, and Se atoms. In the case of the above-mentioned tetrapyrazinoporphyrazine macrocycle (Figure 1A), a $\sigma-\pi$ electron withdrawing effect from the central porphyrazine core to the periphery of the macrocycle is due to the presence of the N atoms of the annulated pyrazine rings. As has been quite recently shown,[5] an electron withdrawing effect is additionally contributed by the pyridine rings appended to the pyrazine rings of the macrocycle. This has been evidenced by the remarkable acid strength of the central NH groups of the free-base ligand[5a] and by the capability of the macrocycle to electrochemically undergo reversible multistep reduction processes at extremely positive potentials.

The possibility to quaternize the pyridine N atoms in the novel series of pyrazinoporphyrazine macrocycles[5] was considered not only as a means of providing water-soluble materials but also of potential interest for studies in the area of biochemistry.[1,3] The quaternization reaction was also postulated as a process capable of enhancing a further peripheral displacement of electronic charge within the macrocyclic framework, with effects being seen on the dissociation properties of the central NH groups in the unmetalated macrocycle and on the reduction properties of the entire series of new macrocycles. In a previous report,[6] it was shown that quaternization of the pyridine N atoms on octapyridinoporphyrazine $[Py_8PzH_2]$, a macrocycle carrying eight pyridine rings directly attached to the β carbon atoms of the central pyrrol rings, leads to formation of a corresponding "supercharged" octakis(*N*-methyl-4-pyridiniumyl)-porphyrazine, $[(4\text{-Mepy})_8PzH_2]^{8+}$. This cationic macrocycle, studied in detail,[6] was shown to undergo, in water (0.1 M NaCl, 0.01 M buffer phosphate), two distinct deprotonation processes with associated pK_a values of 4.1 and 5.6, indicated as the highest values ever found in the field of porphyrins and tetraazaporphyrins.

The present contribution reports on the hydrated iodide salt of the octacationic porphyrazine macrocycle shown in Figure 1B, i.e., tetrakis-2,3-[5,6-di{2-(*N*-methyl)pyridiniumyl}-pyrazino]porphyrazine. The neutral species, abbreviated as $[(2\text{-Mepy})_8TPyzPzH_2](I_8)\cdot 8H_2O$ (2-Mepy = 2-(*N*-methyl)-pyridiniumyl fragment), was obtained from its corresponding Mg^{II} complex, $[(2\text{-Mepy})_8TPyzPzMg(H_2O)](I_8)\cdot 5H_2O$, this latter species being easily prepared by full quaternization at the pyridine N atoms of the macrocyclic Mg^{II} precursor $[Py_8TPyzPzMg(H_2O)]\cdot 4H_2O$[5b] via a reaction with CH_3I in *N*,*N*-dimethylformamide (DMF). The solid state and solution studies presented here provide information on the general physicochemical properties of the neutral unmetalated species $[(2\text{-Mepy})_8TPyzPzH_2](I_8)\cdot 8H_2O$ and on the electronic effects caused by the quaternization process at the pyridine N atoms of the octacationic fragment $[(2\text{-Mepy})_8TPyzPzH_2]^{8+}$. The synthesis and physicochemical characterization of

(4) (a) Stuzhin, P. A.; Bauer, E. M.; Ercolani, C. *Inorg. Chem.* **1998**, *37*, 1533. (b) Bauer, E. M.; Cardarilli, D.; Ercolani, C.; Stuzhin, P. A.; Russo, U. *Inorg. Chem.* **1999**, *38*, 6114. (c) Bauer, E. M.; Ercolani, C.; Galli, P.; Popkova, I. A.; Stuzhin, P. A. *J. Porphyrins Phthalocyanines* **1999**, *3*, 371. (d) Angeloni, S.; Bauer, E. M.; Ercolani, C.; Popkova, I. A.; Stuzhin, P. A. *J. Porphyrins Phthalocyanines* **2001**, *5*, 881. (e) Donzello, M. P.; Ercolani, C.; Stuzhin, P. A.; Chiesi-Villa, A.; Rizzoli, C. *Eur. J. Inorg. Chem.* **1999**, 2075. (f) Donzello, M. P.; Dini, D.; D'Arcangelo, G.; Ercolani, C.; Zhan, R.; Ou, Z.; Stuzhin, P. A.; Kadish, K. M. *J. Am. Chem. Soc.* **2003**, *125*, 14190. (g) Kudrik, E. V.; Bauer, E. M.; Ercolani, C.; Stuzhin, P. A.; Chiesi-Villa, A.; Rizzoli, C. *Mendeleev Commun.* **2001**, 45. (h) Donzello, M. P.; Ercolani, C.; Gaberkorn, A. A.; Kudrik, E. V.; Meneghetti, M.; Marcolongo, G.; Rizzoli, C.; Stuzhin, P. A. *Chem.-Eur. J.* **2003**, *9*, 4009.

(5) (a) Donzello, M. P.; Ou, Z.; Monacelli, F.; Ricciardi, G.; Rizzoli, C.; Ercolani, C.;Kadish, K. M. *Inorg. Chem.* **2004**, *43*, 8626. (b) Donzello, M. P.; Ou, Z.; Dini, D.; Meneghetti, M.; Ercolani, C.; Kadish, K. M. *Inorg. Chem.* **2004**, *43*, 8637.

(6) Anderson, M. E.; Barrett, A. G. M.; Hoffman, B. M. *Inorg. Chem.* **1999**, *38*, 6143.

the metal derivatives of this positively charged macrocycle isolated as hydrated iodide salts of the general formula [(2-Mepy)$_8$TPyzPzM](I$_8$)·xH$_2$O (M = Mg^{II}(H$_2$O), Co^{II}, Cu^{II}, Zn^{II}; x = 2−5) are presented in the following companion paper.[7]

Experimental Section

Solvents and reagents were used as received, unless otherwise specified. Anhydrous tetrahydrofuran (THF) was prepared by refluxing it over potassium and then distilled before use. Pyridine was dried by refluxing over CaO. Dimethyl sulfoxide (DMSO) was freshly distilled over CaH$_2$. Diaminomaleonitrile and 2,2′-pyridil were purchased from Aldrich and used without further purification. The synthesis of 2,3-dicyano-5,6-di(2-pyridyl)-1,4-pyrazine, [(CN)$_2$Py$_2$Pyz], was carried out as reported previously.[5a] The unmetalated macrocycle tetrakis-2,3-[5,6-di(2-pyridyl)pyrazino]-porphyrazine bis-hydrate, [Py$_8$TPyzPzH$_2$]·2H$_2$O, prepared by direct cyclotetramerization of [(CN)$_2$Py$_2$Pyz] in the presence of 1,8-diazabicyclo[5.4.0]undec-7-ene (DBU),[5a] and its Mg^{II} derivative, [Py$_8$TPyzPzMg(H$_2$O)]·4H$_2$O,[5b] were obtained by previously described procedures.

Synthesis of [(CN)$_2$Py(2-Mepy)Pyz](I) (1). [(CN)$_2$Py$_2$Pyz] (289.3 mg, 1.02 mmol) and CH$_3$I (0.725 mL, 11.6 mmol) were dissolved in DMF (3 mL). The obtained yellow-amber solution was kept at room temperature for 4 days. After addition of ether (5 mL), the final dark red solution was kept in a refrigerator overnight. A yellow-orange crystalline material was formed and was separated from the solution, washed repeatedly with ether, and brought to constant weight under vacuum (390 mg, mp 230−233 °C; yield 53%). Calcd for [(CN)$_2$Py(2-Mepy)Pyz](I) (**1**), C$_{17}$H$_{11}$IN$_6$: C, 47.89; H, 2.60; N, 19.72. Found: C, 47.81; H, 2.64; N, 19.34%. IR (cm^{-1}) (KBr): 3420 broad vw, 3140 vvw, 3080 w, 3020 w, 2930 vw, 2230 w, 1660 vw, 1625 ms, 1585 s, 1565 vvw, 1520 ms, 1470 vw, 1460 wm, 1435 w, 1405 wm, 1380 s, 1320 w, 1280 ms, 1265 wm, 1245 wm, 1220 wm, 1195 vvw, 1185 m, 1175 m, 1155 vvw, 1140 wm, 1130 wm, 1085 m, 1045 w, 1000 ms, 955 w, 905 vvw, 820 ms, 775 s, 755 m, 745 ms, 705 w, 685 wm, 665 m, 625 wm, 610 w, 585 m, 550 w, 520 wm, 500 w, 460 w, 440 wm, 425 wm, 410 wm, 385 wm, 325 m. ^{1}H NMR (DMSO-d_6, 293 K): δ/ppm = 9.31 (d, J = 6.0 Hz, 1H), 8.69 (t, J = 7.2, 8.1 Hz, 1H), 8.47 (d, J = 8.1 Hz, 1H), 8.34 (t, J = 6.9, 6.9 Hz, 1H), 8.28 (d, J = 4.8 Hz, 1H), 8.13 (t, J = 7.2, 7.8 Hz, 1H), 8.05 (d, J = 8.1 Hz, 1H), 7.57 (t, J = 5.4, 6.3 Hz, 1H), 4.18 (s, 3H). Suitable crystals of the species were used for single-crystal X-ray work (see below).

Synthesis of [(CN)$_2$Py(2-Mepy)Pyz](OTs) (2). [(CN)$_2$Py$_2$Pyz] (392 mg, 1.37 mmol) and methyl *p*-toluenesulfonate (MeOTs; 0.5 mL, 3.31 mmol, molar ratio 1:2) were dissolved in DMF (3 mL), and the solution was kept at 160 °C for 4 h. After cooling and addition of acetone, the brown crystalline material formed was separated, washed with cold acetone, and brought to constant weight under vacuum (303 mg, mp 185−190 °C; yield 45%). Calcd for [(CN)$_2$Py(2-Mepy)Pyz](OTs) (**2**) C$_{24}$H$_{18}$N$_6$O$_3$S: C, 59.01; H, 4.13; N, 17.20; S, 6.56. Found: C, 59.57; H, 3.89; N, 16.87; S, 6.46%. IR (cm^{-1}) (KBr): 3440 broad wm, 3088 vw, 3050 vw, 3030 w, 3020 wm, 3010 m, 2920 vvw, 2840 vvw, 2240 vw, 1980 w, 1920 w, 1815 vvw, 1710 w, 1670 w, 1630 s, 1600 vw, 1570 s, 1525 s, 1495 m, 1455 s, 1420 m, 1400 s, 1380 vs, 1330 vvw, 1310 vvw, 1285 m, 1280 wm, 1245 s, 1215 vs, 1200 vs, 1180 vs, 1160 w, 1140 w, 1120 vs, 1090 s, 1055 vvw, 1020 vs, 1010 vs, 1000 wm, 975 vw, 950 w, 850 w, 820 s, 805 m, 785 vs, 760 vvw, 750 m, 710 vw, 705 vw, 675 vs, 665 vvw, 620 wm, 610 vw, 575 w, 565 vs, 550 vvw, 525 m, 495 vvw, 445 w, 425 w, 410 vvw, 395 wm, 370 wm, 330 m, 290 vvw. ^{1}H NMR (DMSO-d_6, 293 K): δ/ppm 9.28 (d, J = 5.7 Hz, 1H), 8.66 (t, J = 7.2, 7.8 Hz, 1H), 8.44 (d, J = 8.1 Hz, 1H), 8.30 (t, J = 6.9, 7.2 Hz, 1H), 8.24 (d, J = 3.9 Hz, 1H), 8.11 (t, J = 7.5, 8.1 Hz, 1H), 8.02 (d, J = 8.1 Hz, 1 H), 7.55 (t, J = 6.0, 6.3 Hz, 1H), 7.42 (d, J = 6.3 Hz, 2H), 7.08 (d, J = 8.7 Hz, 2H), 4.15 (s, 3H), 2.27 (s, 3H). Suitable crystals of this compound were used for single-crystal X-ray work (see below).

Synthesis of [(CN)$_2$(2-Mepy)$_2$Pyz](OTs)$_2$·4H$_2$O. [(CN)$_2$Py$_2$Pyz] (587.9 mg, 2.07 mmol) and MeOTs (2 mL, 13.25 mmol; molar ratio 1:6) were dissolved in DMF (5 mL), and the solution was kept at 100 °C for 1−2 days. After cooling and addition of water (5 mL), thin long beige colored needles were formed on standing (2−3 days). The crystalline material was separated by filtration, washed with water and acetone, and brought to constant weight under vacuum (1.04 g; mp 150−155 °C; yield 70%). Calcd for [(CN)$_2$(2-Mepy)$_2$Pyz](OTs)$_2$·4H$_2$O, C$_{32}$H$_{36}$N$_6$O$_{10}$S$_2$: C, 52.74; H, 4.98; N, 11.53; S, 8.80. Found: C, 52.84; H, 4.78; N, 11.57; S, 8.06%. Thermogravimetric analysis shows a weight loss (H$_2$O) from room temperature up to 130 °C (calcd for four molecules of water: 9.89; found: 9.45%). IR (cm^{-1}) (KBr): 3600 ms, 3540 ms, 3460 s, 3380 s, 3260 ms, 3140 vvw, 3080 ms, 3050 ms, 3030 ms, 2920 vvw, 2560 vvw, 2340 vvw, 2240 vvw, 1940 vw, 1840 vvw, 1650 ms, 1630 s, 1600 w, 1535 m, 1520 m, 1495 m, 1450 m, 1410 vvw, 1385 s, 1310 vw, 1305 vw, 1290 ms, 1250 vvw, 1210 vs, 1190 vs, 1180 vs, 1120 vs, 1070 ms, 1030 vs, 1010 vs, 950 w, 895 vvw, 870 w, 860 w, 830 ms, 825 ms, 810 vw, 800 wm, 780 ms, 755 wm, 730 vvw, 710 vvw, 690 vs, 640 vvw, 600 vvw, 570 vs, 550 vvw, 525 w, 470 vvw, 440 m, 400 m, 370 m, 335 m, 310 vvw, 300 m, 255 vvw, 240 vvw. ^{1}H NMR (DMSO-d_6, 293 K): δ/ppm 9.33 (d, J = 6.3 Hz, 2H), 8.50 (t, J = 8.1, 7.2 Hz, 2H), 8.27 (t, J = 7.2, 6.9 Hz, 2H), 8.05 (d, J = 7.5 Hz, 2H), 7.44 (d, J = 6.3 Hz, 4H), 7.10 (d, J = 8.1 Hz, 4H), 4.37 (s, 6H), 2.28 (s, 6H). Attempts to obtain single crystals of this compound gave only very thin white needles unsuitable for single-crystal X-ray work.

Tetrakis-2,3-[5,6-di{2-(*N*-methyl)pyridiniumyl}pyrazino]-porphyrazinato(monoaquo)magnesium(II) Octaiodide Pentahydrate, [(2-Mepy)$_8$TPyzPzMg(H$_2$O)](I$_8$)·5H$_2$O. The Mg^{II} complex [Py$_8$TPyzPzMg(H$_2$O)]·4H$_2$O (58.3 mg, 0.041 mmol) and CH$_3$I (0.7 mL, 11.24 mmol) were added to DMF (1 mL), and the mixture was kept under stirring at room temperature for 4 days. After evaporation of the methyl iodide, the brilliant green solid material was separated by centrifugation, washed with benzene and ether, and brought to constant weight under vacuum (43 mg). More material was separated (50.2 mg) on addition of benzene (2 mL) to the DMF solution which was left to stand for 2 days (total yield: ca. 50%). Calcd for [(2-Mepy)$_8$TPyzPzMg(H$_2$O)](I)$_8$·5H$_2$O, C$_{72}$H$_{68}$I$_8$MgN$_{24}$O$_6$: C, 35.96; H, 2.85; N, 13.98. Found: C, 36.70; H, 3.12; N, 14.50%. IR (cm^{-1}) (KBr): 3395 broad s, 3208 sh, 3142 vvw, 3081 w, 3049 w, 3007 w, 2926 vvw, 2756 w, 1660 ms, 1624 s, 1583 s, 1554 w, 1519 ms, 1485 ms, 1457 ms, 1438 w, 1407 w, 1383 w, 1359 s, 1318 vvw, 1282 wm, 1247 vs, 1192 s, 1147 w, 1111 s, 1091 wm, 1041 vw, 1022 vw, 998 m, 955 ms, 889 vw, 866 w, 828 w, 797 sh, 782 wm, 749 wm, 719 wm, 703 s, 659 wm, 637 vvw, 627 w, 602 vvw, 570 wm, 534 vw, 511 vw, 473 vvw, 442 m. Thermogravimetric analysis showed a 3.8% weight loss of H$_2$O from room temperature up to 130 °C (calcd for 5H$_2$O: 3.74%).

Tetrakis-2,3-[5,6-di{2-(*N*-methyl)pyridiniumyl}pyrazino]-porphyrazine Octaiodide Octahydrate, [(2-Mepy)$_8$TPyzPzH$_2$](I$_8$)·8H$_2$O from the Corresponding Mg^{II} Complex. The complex [(2-Mepy)$_8$TPyzPzMg(H$_2$O)](I$_8$)·5H$_2$O (65 mg, 0.027 mmol) was suspended in 0.6 M HCl (0.7 mL), and the mixture was

(7) Bergami, C.; Donzello, M. P.; Ercolani, C.; Monacelli, F.; Kadish, K. M. *Inorg. Chem.* **2005**, *44*, 9862−9873.

kept under stirring at room temperature for 1 h. The solid was separated by filtration, washed with a few drops of water to neutralization, and dried under vacuum (39.8 mg; 61%). Calcd for $[(2\text{-Mepy})_8\text{TPyzPzH}_2](I_8)\cdot 8H_2O$, $C_{72}H_{74}I_8N_{24}O_8$: C, 35.75; H, 3.08; N, 13.90; I, 41.97. Found: C, 35.27; H, 2.38; N, 14.28; I, 41.74%. Thermogravimetric analysis indicated a weight loss (H_2O) of 5.70% (calcd for eight molecules of water: 5.96%). IR (cm^{-1}) (KBr): 3400 (broad) w, 1780 w, 1740 m, 1680 broad wm, 1621 m, 1581 m, 1555 wm, 1539 w, 1515 wm, 1505 wm, 1472 w, 1455 w, 1430 w, 1401 wm, 1388 w, 1354 m, 1311 w, 1275 w, 1261 w, 1239 wm, 1176 w, 1141 wm, 1099 w, 1091 w, 1065 vw, 1043 vw, 1015 vw, 997 m, 949 m, 825 wm, 769 m, 745 m, 717 wm, 690 m, 661 vw, 645 w, 627 w, 614 vvw, 596 w, 577 vw, 566 w, 560 vw, 532 vw, 528 vw, 500 vvw, 488 vvw, 475 vvw, 461 vvw, 435 w, 416 w, 405 w.

Tetrakis-2,3-[5,6-di{2-(*N*-methyl)pyridiniumyl}pyrazino]-porphyrazine Octachloride Hexadecahydrate, $[(2\text{-Mepy})_8\text{TPyzPzMg}(H_2O)](Cl_8)\cdot 16H_2O$, from the Related Iodide and Its Demetalation to the Corresponding Free-Base Macrocycle. Resin Amberlite IRA-400 (1.11 g) was used for preparation of a small chromatographic column which was first washed with H_2O, then with 0.5 M NaOH, H_2O, 2.0 M HCl, and finally with water until the solution was neutral. A solution of 2.2×10^{-3} M $[(2\text{-Mepy})_8\text{TPyzPzMg}(H_2O)](I_8)\cdot 5H_2O$ (42.3 mg, 0.018 mmol) in distilled water (8 mL) was then passed through the column. The eluted solution was evaporated to dryness, and the solid was brought to constant weight under vacuum (10 mg, yield 30%). Calcd for $[(2\text{-Mepy})_8\text{TPyzPzMg}(H_2O)](Cl_8)\cdot 16H_2O$, $C_{72}H_{90}Cl_8MgN_{24}O_{17}$: C, 46.21; H, 4.85; N, 17.96. Found: C, 46.24; H, 5.37; N, 18.24%.

$[(2\text{-Mepy})_8\text{TPyzPzMg}(H_2O)](Cl_8)\cdot 16H_2O$ (10 mg, 0.0054 mmol) was dissolved in 0.5 mL of 0.6 N HCl. The solution was kept at room temperature for 40 min and then brought to neutrality with NaOH. After evaporation of water, the obtained solid consisted of a mixture of $[(2\text{-Mepy})_8\text{TPyzPzH}_2](Cl_8)\cdot xH_2O$ and NaCl and was used as such for titration studies (see a short reference to this chloride in the later discussion below).

Titration of $[(2\text{-Mepy})_8\text{TPyzPzH}_2](I_8)\cdot 8H_2O$ in Water Solution. (a) Titration Starting from Strongly Acidic Solutions. A known volume (ca. 20 mL) of a solution of the hydrated neutral species $[(2\text{-Mepy})_8\text{TPyzPzH}_2](I_8)$ (ca. 1×10^{-5} M) in 2 N HCl, containing $Na_3PO_4\cdot 12H_2O$ (0.010 M) was placed in a 1 cm spectrophotometric cell modified so as to contain up to 40 mL of solution and provided with inlets for a glass electrode and for the injection of reagents. The cell was placed in the cell compartment of the spectrophotometer, and its temperature was controlled at 20.0 °C by circulating water from a thermostat. A titration procedure was followed by gradually adding to the solution microvolumes of a concentrated NaOH solution up to a final pH value of 11. The pH and the UV−visible spectrum of the solution were measured after each addition.

(b) Titrations Starting from Basic Solutions Cycled in the pH Range 11−1.4. A known volume (ca. 20 mL) of a water solution of hydrated $[(2\text{-Mepy})_8\text{TPyzPzH}_2](I_8)$ (ca. 1×10^{-5} M), containing $Na_3PO_4\cdot 12H_2O$ (0.010 M) and NaCl (2.0 M), was placed in the same cell described above. Small volumes (1−5 μL) of HCl solutions (1.2 or 6.0 N) were added to the solution so as to gradually bring the pH, initially ca. 11, to a minimum value of 1.4 (*direct titration*). Here too, the pH and the UV−visible spectrum of the solution were systematically measured after each addition. Once the pH reached its programmed minimum value, it was brought back to 11.0 by stepwise addition of microvolumes of a suitably concentrated NaOH solution, again with the pH measured, and the spectrum was taken after each addition (*reverse titration*). After this *first titration cycle*, the entire procedure was then repeated with further additions of HCl and then NaOH so as to process a *second titration cycle*. Some of the titrations were conducted by lowering the pH only down to slightly acidic solutions (pH $\cong$ 4). The volumes of acid and base added were always small enough so that no correction for dilution was needed when comparing the spectra.

Table 1. Experimental Data for the X-ray Diffraction Study on Crystalline Compounds **1** and **2**

compound	$[(CN)_2\text{Py}(2\text{-Mepy})\text{Pyz}](I)$, **1**	$[(CN)_2\text{Py}(2\text{-Mepy})\text{Pyz}](OTs)$, **2**
formula	$C_{17}H_{11}IN_6$	$C_{24}H_{18}N_6O_3S$
a, Å	13.489(3)	14.178(3)
b, Å	13.181(3)	14.442(4)
c, Å	11.005(1)	11.400(2)
β,°	112.38(2)	90
V, Å^3	1808.0(6)	2334.2(9)
Z	4	4
formula weight	426.2	470.5
space group	*Cc*	$P2_12_12_1$
t, °C	25	25
λ, Å	1.54178	1.54178
ρ_{calc}, g cm^{-3}	1.566	1.339
μ, cm^{-1}	139.99	15.58
transm coeff	0.166−0.210	0.563−0.616
R[a]	0.056	0.042
wR2	0.148	0.117
GOF	1.03	1.06
N-observed[b]	1677	3978
N-independent[c]	1756	4428
N-refinement[d]	1728	4348
variables	217	307

[a] Calculated on the observed reflections having $I > 2\sigma(I)$. [b] *N*-observed is the number of the independent reflections having $I > 2\sigma(I)$. [c] *N*-independent is the number of independent reflections. [d] *N*-refinement is the number of reflections used in the refinement having $I > 0$.

(c) Experiments at Constant pH. A Hi-Tech manual stopped-flow accessory connected to a specially designed 1 cm spectrophotometric cell was used to obtain solutions of the iodide salt of $[(2\text{-Mepy})_8\text{TPyzPzH}_2]^{8+}$ at different selected pH values over the range of 10−0.4. The experiments consisted of a virtually instantaneous mixing of two solutions contained in two reservoirs filled with (A) a solution of the above iodide salt (ca. 2×10^{-5} M), $Na_3PO_4\cdot 12H_2O$ (0.020 M), and NaCl (2.0 M) and (B) a NaCl (2.0 M) solution containing the appropriate concentration of HCl. Mixing of the two solutions for each predetermined pH value was followed by an immediate recording of the UV−visible spectrum in the region 560−740 nm, and the changes in spectra were then monitored as a function of time. When the full spectral region could not be explored due to too rapid a change of the spectrum to be followed by our instrumentation (pH < 2), only the absorbance at 625 nm was measured at appropriate time intervals until a constant reading was obtained. The spectrum of the solution obtained by a 1:1 mixing of solution A and a solution containing 2.0 M NaCl (resulting pH = 11.0) was used to normalize the absorbances.

X-ray Crystallography of $[(CN)_2\text{Py}(2\text{-Mepy})\text{Pyz}](I)$ (1) and $[(CN)_2\text{Py}(2\text{-Mepy})\text{Pyz}](OTs)$ (2). Crystal data and details associated with structure refinements for **1** and **2** are given in Table 1 and in the Supporting Information. Data were collected on an Enraf-Nonius CAD4 diffractometer using graphite-monochromatized Cu Kα radiation at 298 K. The solutions and refinements were carried out using the programs SIR97[8] and SHELX97.[9]

(8) Altomare, A.; Burla, M. C.; Camalli, M.; Cascarano, G.; Giacovazzo, C.; Guagliardi, A.; Moliterni, A. G. G.; Polidori, G.; Spagna, R. *J. Appl. Crystallogr.* **1999**, *32*, 115.
(9) Sheldrick, G. M. shelxl97. Program for crystal structure refinement. University of Göttingen, Germany, 1997.

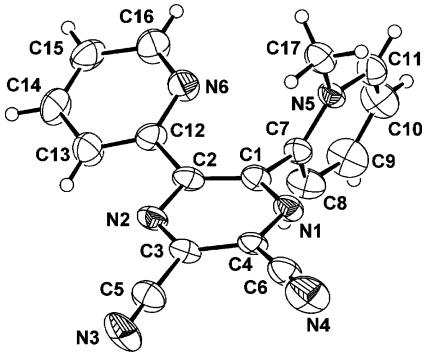

Figure 2. ORTEP side-top view of the cation $[(CN)_2Py(2\text{-}Mepy)Pyz]^+$ in the iodide species (compound **1**).

Other Physical Measurements. IR spectra were taken with a Perkin-Elmer 1760 X spectrophotometer in the range 4000−400 cm^{-1} by using KBr pellets. UV−visible solution spectra were registered with a Varian Cary 5E spectrometer. Thermogravimetric analyses (TGA) were performed on a Stanton Redcroft model STA-781 analyzer under an N_2 atmosphere (0.5 L/min). Elemental analyses for C, H, and N were provided by the "Servizio di Microanalisi" at the Dipartimento di Chimica, Università "La Sapienza" (Rome) on an EA 1110 CHNS-O instrument. Elemental analyses of iodine were obtained from the Analytische Laboratorien (Lindlar, Germany). X-ray powder diffraction patterns were obtained on a Philips PW 1710 diffractometer by using a Cu Kα (Ni-filtered) radiation. ^{1}H NMR spectra were recorded on a 200 MHz Brucker spectrophotometer at the Dipartimento di Chimica, Università "La Sapienza".

Results and Discussion

Structures of $[(CN)_2Py(2\text{-}Mepy)Pyz](I)$ (1) and $[(CN)_2Py(2\text{-}Mepy)Pyz](OTs)$ (2). The structures of **1** and **2** both consist of the packing of the common cation and the different anions in a stoichiometric ratio of 1:1. The ORTEP side-top view of the cation in the iodide species is depicted in Figure 2. Selected bond distances and angles for both compounds are listed in Table 2. Relevant conformation parameters are summarized in the Supporting Information. In the two very similar structures of the cation, the pyrazine ring is slightly distorted, assuming a twist-boat conformation as indicated by the puckering parameters given in Table S1 (Supporting Information). This is like what was observed in the unquaternized species.[5a] The deviations from planarity, calculated in terms of out-of-plane distances from the least-squares plane through the pyrazine ring, range from −0.062(13) to 0.053(10) Å for **1** and from −0.016(3) to 0.021(3) Å for **2**.

Noticeably, methylation of one N atom causes the related pyridine ring in **1** and **2** to be positioned almost perpendicularly with respect to the pyrazine ring (dihedral angle: 75.6(3) and 86.5(1)° for **1** and **2**, respectively), whereas the unquaternized pyridine rings are nearly parallel (dihedral angle: 18.3 and 7.6(1)° for **1** and **2**, respectively).

The two pyridine rings in each species are nearly perpendicular to one another, the dihedral angles formed by the N6,C12..C16 and N5,C7..C11 rings being 76.2(4) and 86.5(1)° in **1** and **2**, respectively. The trend of the bond distances within the pyrazine rings is consistent with a complete delocalization of the double bond system. In the crystal packing intra- and intermolecular contacts could be interpreted in terms of weak hydrogen interactions, the shortest ones being as follows:

Compound **1**: C9...N3′, 3.371(19) Å; C17...N3″, 3.45(2) Å; H172...N3″, 2.66 Å; C17−H172...N3″, 140.4°; C16...N4″, 3.34(2) Å; H16...N4″, 2.58 Å; C16−H16...N4″, 140.3° (prime and double prime refer to transformations of x, y, $1 + z$ and $0.5 + x$, $0.5 - y$, $-0.5 + z$, respectively).

Compound **2**: C8...O1, 3.247(4) Å; H8...O1, 2.32 Å; C8−H8...O1, 174.1°; C9...N3′, 3.396(4) Å; H9...N3′, 2.75 Å; C9−H9...N3′, 127.4°; C17...O2″, 2.561(4) Å; H17...O2″, 2.56 Å; C17−H17...O2″, 152.2°; C11...O2″, 3.094(4) Å; H11...O2″, 2.20 Å; C11−H11...O2″, 160.8° (prime and double prime refer to transformations of $0.5 + x$, $0.5 - y$, $1 - z$ and $0.5 - x$, $1 - y$, $-0.5 + z$, respectively).

$[(2\text{-}Mepy)_8TPyzPzH_2](I_8)\cdot 8H_2O$ Synthetic Aspects. The iodide salt $[(2\text{-}Mepy)_8TPyzPzH_2](I_8)\cdot 8H_2O$ (hereafter water neglected) was prepared by demetalation of the corresponding Mg^{II} complex (see the Experimental Section), since attempts at direct full methylation of the corresponding neutral free-base macrocycle $[Py_8TPyzPzH_2]$ by using CH_3I, methyl *p*-toluenesulfonate, or trimethyloxonium tetrafluoroborate as a methylating agent gave always mixtures of differently quaternized materials with average values of 5−6 methylated N atoms per macrocyclic unit. Moreover, procedures which used the diquaternized *p*-toluenesulfonate $[(CN)_2(2\text{-}Mepy)_2Pyz](OTs)_2\cdot 4H_2O$ in an autocyclotetramerization process or the metal template reactions with Mg^{II} propylate or amylate gave unsatisfactory results. The chlatrated water, which was variable from sample to sample in the above iodide compound, could be easily eliminated by heating (100 °C) under vacuum. Exposure to air led to

Table 2. Selected Bond Distances (Å) and Angles (deg) for Compounds **1** and **2**

	$[(CN)_2Py(2\text{-}Mepy)Pyz](I)$, **1**	$[(CN)_2Py(2\text{-}Mepy)Pyz](OTs)$, **2**
N(1)−C(1)	1.353(14)	1.325(3)
N(1)−C(4)	1.333(18)	1.335(3)
N(2)−C(2)	1.341(18)	1.336(2)
N(2)−C(3)	1.320(15)	1.327(3)
N(3)−C(5)	1.14(3)	1.133(4)
N(4)−C(6)	1.12(2)	1.137(4)
C(1)−C(2)	1.388(12)	1.416(3)
C(1)−C(7)	1.461(16)	1.507(2)
C(2)−C(12)	1.492(15)	1.480(3)
C(3)−C(4)	1.408(13)	1.392(3)
C(3)−C(5)	1.440(18)	1.454(3)
C(4)−C(6)	1.441(17)	1.441(4)
C(1)−N(1)−C(4)	116.9(9)	116.7(2)
C(2)−N(2)−C(3)	115.4(10)	117.7(2)
N(1)−C(1)−C(2)	120.4(8)	122.6(2)
N(1)−C(1)−C(7)	114.4(9)	112.8(2)
C(2)−C(1)−C(7)	124.9(8)	124.4(1)
N(2)−C(2)−C(1)	122.6(9)	119.6(1)
N(2)−C(2)−C(12)	115.8(10)	116.6(2)
C(1)−C(2)−C(12)	121.6(8)	123.8(2)
N(2)−C(3)−C(4)	122.9(9)	122.1(2)
N(2)−C(3)−C(5)	117.2(10)	117.5(2)
C(4)−C(3)−C(5)	119.9(9)	120.3(2)
N(1)−C(4)−C(3)	120.5(9)	121.2(2)
N(1)−C(4)−C(6)	118.2(10)	117.5(2)
C(3)−C(4)−C(6)	121.3(8)	121.3(2)
N(3)−C(5)−C(3)	175.6(15)	178.0(3)
N(4)−C(6)−C(4)	177.4(13)	178.5(3)

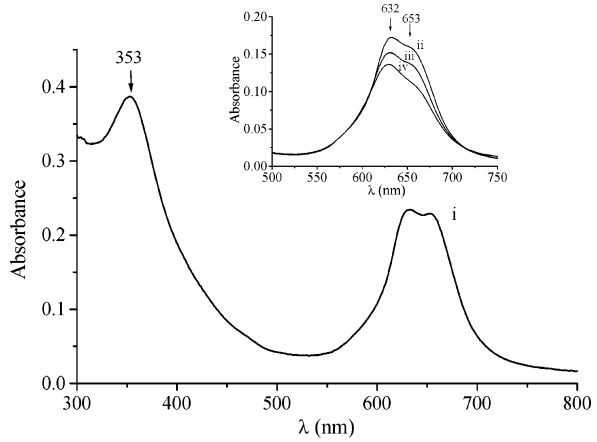

Figure 3. UV−visible spectrum of the cation $[(2\text{-Mepy})_8\text{TPyzPzH}_2]^{8+}$ in water (i). The inset shows the spectral evolution of the Q-band region of the spectrum (which shows no changes as a function of time) upon addition of NaCl to solution (ii = 0.1 M; iii = 1.0 M; iv = 2.0 M).

rehydration of the species. The X-ray powder pattern shows that the material is an essentially amorphous solid, either in its hydrated or anhydrous form.

UV−Visible Spectral Features of Hydrated $[(2\text{-Mepy})_8\text{TPyzPzH}_2](I_8)$ in Neutral, Acidic, or Basic Water Solutions and in Low-Donor Organic Solvents. The title compound is sparingly soluble in pure water, but its solubility depends on the pH value and changes under different experimental conditions (buffer, ionic strength), this implying different formulations for the macrocyclic cationic component. This is discussed below.

Neutral Water. Upon contact of $[(2\text{-Mepy})_8\text{TPyzPzH}_2](I_8)$ with pure water, a cloudy dispersion is initially formed, slowly turning to a clear solution which shows a broad UV−visible absorption envelope in the spectral Q-band region having two maximum intensity peaks of round contour at 632 and 653 nm, suggesting some form of aggregation (Figure 3i). Only a slight decrease in intensity of the spectrum was observed over a 3 h period. Moreover, no changes in the spectrum were observed upon diluting the solution over the range $1 \times 10^{-5}-1 \times 10^{-7}$ M (see Table 3 for the ϵ values). Noticeably, the spectrum shows some dependence upon ionic strength as seen in Figure 3 (inset). As described below, the spectrum belongs to an aggregated form of the cation $[(2\text{-Mepy})_8\text{TPyzPzH}_2]^{8+}$ (possibly partially deprotonated). Indeed, aggregation seems to characterize the behavior of the present macrocycle in water solutions, either in its octacationic form $[(2\text{-Mepy})_8\text{TPyzPzH}_2]^{8+}$ or as the deprotonated species $[(2\text{-Mepy})_8\text{TPyzPz}]^{6+}$. Aggregation, a commonly observed feature of phthalocyanine[10] and porphyrazine systems,[3] may be favored in this case by the planarity of the central π-conjugated porphyrazine framework which is expanded to include the annulated pyrazine rings. Unlike the currently investigated macrocycle, the octacationic porphyrazine macrocycle $[(4\text{-Mepy})_8\text{PzH}_2]^{8+}$, the most pertinent and unique reference material to be mentioned, has a more restricted planar π-conjugated core.[6] This macrocyclic unit is present in its monomeric form over a large range of pH values in water (Cl^- as a counterion),[6] either unmodified or as a centrally deprotonated species $[(4\text{-Mepy})_8\text{Pz}]^{6+}$.

Titration studies of $[\text{Py}_8\text{TPyzPzH}_2]$ in CH_2Cl_2 with TBA(OH) have proven that this macrocycle behaves as a strong acid as a result of the electron withdrawing effects caused by the peripheral "dipyridinopyrazine" fragments of the macrocycle.[5a] As to the present octacationic macrocycle $[(2\text{-Mepy})_8\text{TPyzPzH}_2]^{8+}$, studies in water do not allow a precise estimation of the pK_a values owing in large part to the presence of aggregation. Nevertheless, data presented here (see below) provide useful information about the high tendency of the 8+ charged macrocycle to exist in its deprotonated form.

Acidic Solutions. Figure 4 (solid line) shows the spectrum of the octacation $[(2\text{-Mepy})_8\text{TPyzPzH}_2]^{8+}$ dissolved as the iodide salt in aqueous 6.0 N HCl (a quite similar spectrum is also observed in 2.0 N HCl; Table 3).

The presence in the spectrum of a split Q band with peaks at 668 and 684 nm, accompanied by the typical vibrational satellites on the blue side, strongly suggests a D_{2h} symmetry for the porphyrazine core. This excludes further protonation of the inner N_4 chromophore and formation of the species $[(2\text{-Mepy})_8\text{TPyzPzH}_4]^{10+}$.

Moreover, the overall appearance of the spectrum in the range 300−800 nm clearly indicates the absence of aggregation phenomena; thus, at high proton concentrations the octacation is present exclusively in its monomeric centrally protonated form. It should be kept in mind, however, that a formulation of the compound in solution as $[(2\text{-Mepy})_8\text{TPyzPzH}_2]^{8+}$ is indeed not rigorously correct, if account is taken that, under the above-defined strongly acidic conditions (6.0 or 2.0 N HCl), the eight pyrazine N atoms can be assumed to be fully protonated and the *meso* N atoms might also undergo some form of proton interaction. Plausibly, such a high concentration of positive charge on the macrocycle may prevent interunit interaction and aggregation. Noteworthy, these effects seem to have little influence on the symmetry of the π-conjugated porphyrazine core as indicated by the measured spectra (Figure 4, Table 3).

The inset of Figure 4 shows spectra, in the region 500−800 nm, for the corresponding unquaternized species, $[\text{Py}_8\text{TPyzPzH}_2]$, in aqueous 6.0 N HCl (solid line, peaks at 668 and 687 nm) and in CF_3COOH (dashed line, peaks at 658 and 682 nm). Similar to what is seen for cationic $[(2\text{-Mepy})_8\text{TPyzPzH}_2]^{8+}$, here the spectrum shows a split Q band indicative of D_{2h} symmetry. Moreover, the general features of the spectra in the more extended region (300−800 nm) provide no evidence for the presence of molecular aggregation. If it is considered that under strongly acidic conditions all of the pyridine N atoms are protonated, the macrocycle is then more correctly formulated as the monomeric cation $[(\text{HPy})_8\text{TPyzPzH}_2]^{8+}$ (neglecting protonation of the pyrazine rings and proton interaction with the *meso* N atoms). The peak positions of the split Q band (668 and 687 nm) are practically coincident with bands observed for the alkylated analogue $[(2\text{-Mepy})_8\text{TPyzPzH}_2]^{8+}$ (λ_{max} = 668 and 684 nm), thus suggesting that formation of the 1+ charged pyridine

(10) Snow, A. W. *The Porphyrin Handbook*; Kadish, K. M., Smith, K. M., Guilard, R., Eds.; Academic Press: New York, 2003; Vol. 17, Chapter 109, pp 129−176.

Table 3. UV−Visible Spectral Data for Hydrated $[(2\text{-Mepy})_8\text{TPyzPzH}_2](I_8)$ in Different Media

	λ [nm] (log ϵ)						
solvent	Soret region			Q-band region			
H_2O[a]	353 (4.49)					632 (4.26)	655 (4.33)
HCl 2 N[b]	366 (4.55)			610 (sh) (4.12)	614 (sh) (4.16)	669 (4.71)	684 (4.74)
H_2O (pH 11)[c]	351 (4.75)		475 (3.87)		613 (4.19)	666 (3.99)	708 (3.99)
Py[d]	362 (4.87)				617 (sh)	645 (4.60)	675 (4.70)
DMSO[d]	358 (4.86)	414 (sh) (4.60)	464 (sh) (4.14)		618 (4.24)	638 (sh) (4.34)	671 (4.97)
DMF[d]	359 (4.88)	402 (4.69)	474 (4.06)		610 (4.26)	635 (4.37)	672 (4.94)
CH_3CN[d,e]	358	470			600	630 (sh)	665
C_6H_5CN[d,e]	364				609	642 (sh)	677
CH_3OH[d,e]	355				610 (sh)	637 (sh)	666

[a] Aggregated $[(2\text{-Mepy})_8\text{TPyzPzH}_2]^{8+}$. [b] Monomeric $[(2\text{-Mepy})_8\text{TPyzPzH}_2]^{8+}$. [c] Aggregated $[(2\text{-Mepy})_8\text{TPyzPz}]^{6+}$. [d] Monomeric $[(2\text{-Mepy})_8\text{TPyzPz}]^{6+}$. [e] Qualitative spectra.

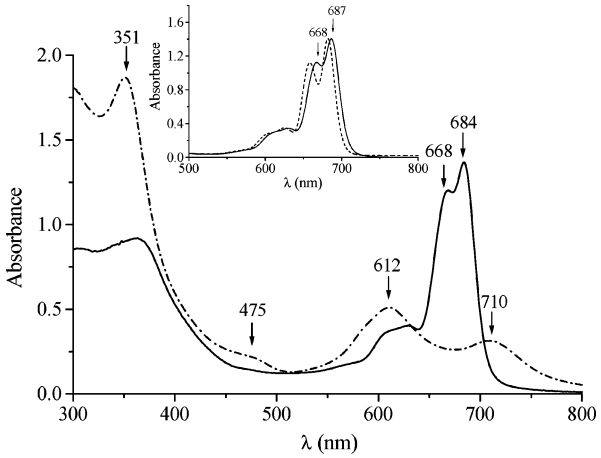

Figure 4. UV−visible spectra of $[(2\text{-Mepy})_8\text{TPyzPzH}_2]^{8+}$ ($c \sim 10^{-5}$ M) in 6.0 N aqueous HCl (solid line) and in a buffered water solution at pH 11 (0.01 M $Na_3PO_4 \cdot 12H_2O$, 2.0 M NaCl, dashed line) The inset shows spectra of the corresponding unquaternized species $[Py_8\text{TPyzPzH}_2]$ in 6.0 N HCl (solid line) and in CF_3COOH (dash−dotted line).

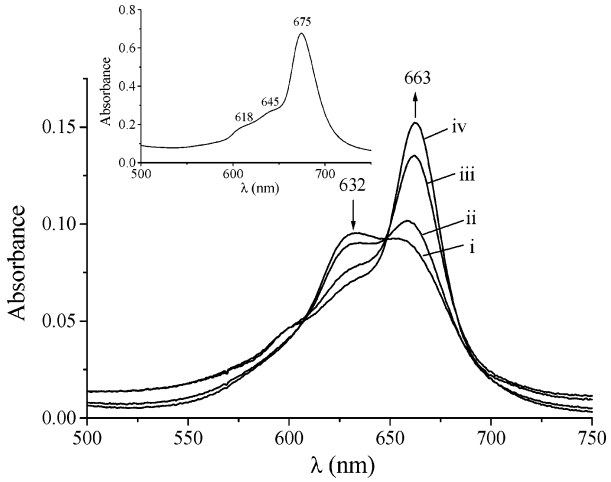

Figure 5. UV−visible spectral changes caused by the progressive addition of pyridine to a water solution of aggregated $[(2\text{-Mepy})_8\text{TPyzPzH}_2]^{6+}$: i, pure water; ii, iii, and iv water/pyridine mixtures containing 8, 18, and 26% py, respectively. The inset shows the spectrum of $[(2\text{-Mepy})_8\text{TPyzPzH}_2]^{6+}$ in neat pyridine.

N atoms results in a similar electronic effect within the macrocycle, no matter what the quaternizing moiety (H or CH_3).

Basic Solutions. The initial spectrum of a buffered water solution of the iodide salt $[(2\text{-Mepy})_8\text{TPyzPzH}_2](I_8)$ at pH 11 (0.01 M $Na_3PO_4 \cdot 12H_2O$, 2.0 M NaCl) is also depicted in Figure 4 (dash−dotted line; data in Table 3). Two broad absorptions appear in the Q-band region with maxima at 612 and 710 nm, and an intense peak is seen in the B-band region at 351 nm plus a broad low intensity absorption at ca. 475 nm. Due to the level of basicity of the medium, and taking into account the above comments about the tendency of the central NH groups to release protons, it is reasonably assumed that the spectrum in Figure 4 belongs to the deprotonated cation $[(2\text{-Mepy})_8\text{TPyzPz}]^{6+}$ most likely present in an aggregated form, as strongly suggested by the broad-shaped absorptions in the Q-band region.

The monomeric form of the deprotonated cation $[(2\text{-Mepy})_8\text{TPyzPz}]^{6+}$ can be observed under different experimental conditions and solvents. Figure 5 shows the spectral changes caused by the progressive addition of pyridine to a water solution of aggregated $[(2\text{-Mepy})_8\text{TPyzPzH}_2]^{8+}$. In a pyridine/water mixture containing 26% pyridine, the spectrum shows only an unsplit Q band accompanied by the usually observed vibrational satellites, while the band at 632 nm is no longer present. The shape of this spectrum is practically identical to that shown by the same species in pure pyridine (Figure 5, inset) and indicates D_{4h} symmetry. This suggests that the addition of pyridine, while facilitating disaggregation, causes central deprotonation of the octacationic macrocycle with formation of the monomeric species $[(2\text{-Mepy})_8\text{TPyzPz}]^{6+}$. These results are not surprising, since they parallel those already observed for the unquaternized species $[Py_8\text{TPyzPzH}_2]$ in a CH_2Cl_2/pyridine mixture and in neat pyridine.[5a] Noteworthy, a spectrum nearly identical to that obtained in pyridine and fully compatible with the presence of the deprotonated cation $[(2\text{-Mepy})_8\text{TPyzPz}]^{6+}$ in its monomeric form is also obtained in DMSO, DMF, CH_3CN, C_6H_5CN, or CH_3OH (Table 3), which demonstrates the tendency of the octacationic macrocycle to undergo disaggregation and deprotonation processes in nonaqueous low-donor solvents. These spectral features are in line with similar behavior observed in the same solvents for the unquaternized $[Py_8\text{TPyzPzH}_2]$, which is converted to its corresponding deprotonated $[Py_8\text{TPyzPz}]^{2-}$ form in the same solvents (see the Supporting Information in ref 5a).

Titration Studies in Water Solutions. Titrations Starting from Strongly Acidic Solutions. As discussed above, the spectra of the octacation $[(2\text{-Mepy})_8\text{TPyzPzH}_2]^{8+}$ in solutions of HCl $\geq$ 2.0 N (Figure 4, Table 3) indicate that it is present in its monomeric protonated form. Figure 6

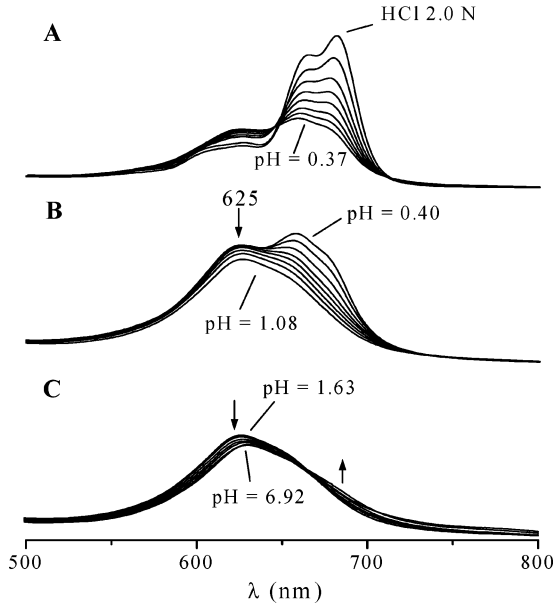

Figure 6. Spectral changes occurring to an acidic solution (2.0 N HCl) of $[(2\text{-Mepy})_8\text{TPyzPzH}_2]^{8+}$ by stepwise microaliquot addition of concentrated NaOH: (A) pH < 0.4, (B) pH range 0.4−1.08, and (C) pH range 1.63−6.92.

illustrates the spectral changes which occur upon stepwise addition of concentrated NaOH to a 2.0 N HCl solution of the octacation (see the Experimental Section). At high acidity values (pH < 0.4, Figure 6A), the split Q band sharply decreases in intensity and a band a ca. 625 nm appears; during these changes an isosbestic point can be seen at 645 nm. In the range of pH 0.4−1.08 (Figure 6B), the split Q band of the monomeric octacation completely disappears, while the 625 nm absorption increases in intensity and appears as an envelope with a shoulder at ca. 650 nm. Both the shape and intensity of this spectral envelope suggest the presence of aggregation. It is therefore plausible that these spectral changes involve deprotonation processes of the pyrazine rings and a weakening of proton interaction with the *meso* N atoms, this resulting in a facilitated aggregation. It should be pointed out that the highly acidic conditions under which the protonation−deprotonation equilibria take place make unreliable conventional pH measurements. This situation prevents quantitative analysis of the absorption data which is needed in order to obtain precise information as to the number of protons involved and the precise nature of the aggregate species in each step.

Upon increasing the pH to about 7 (Figure 6C), the spectrum shows minor changes with the peak at 625 nm slightly shifted to lower energy and a new broad shoulder appearing at ca. 670 nm. This spectrum is practically superimposable with that observed when the free-base macrocycle $[(2\text{-Mepy})_8\text{TPyzPzH}_2]^{8+}$ is directly dissolved (as the iodide salt) in a neutral 2.0 M NaCl water solution (curve iv in Figure 3). Addition of more NaOH causes further modifications, and the final spectrum obtained at pH 11 coincides with what is measured upon direct dissolution of the iodide salt at the same pH value (dash−dotted line in Figure 4) and attributed to the deprotonated aggregated cation $[(2\text{-Mepy})_8\text{TPyzPz}]^{6+}$. Altogether, these observations indicate

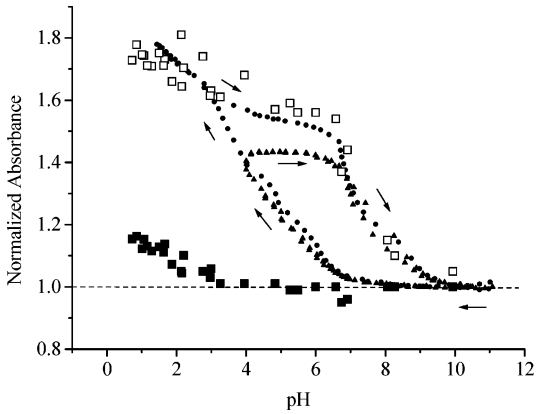

Figure 7. Absorbance values (λ = 625 nm) vs pH measured for the first titration cycles in the pH ranges 11−1.4 (●●●●) and 11−4.0 (▲▲▲▲). Absorbances at 625 nm measured at constant pH immediately after 1:1 mixing of the two solutions (■, see text) and at equilibrium (□).

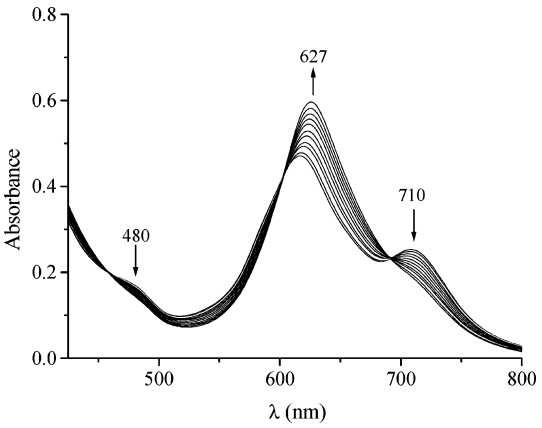

Figure 8. Spectral changes observed during *direct* titration (pH: 11 → 4). Isosbestic points are at 458, 602, and 692 nm.

the existence of a complex sequence of proton transfer equilibria, all involving aggregated species, starting from the monomeric fully protonated moiety found to be present under highly acidic conditions.

Titrations Starting from Basic Solutions and Cycled in the pH Range 11−1.4. The changes of absorbance at 625 nm of the aggregated cation $[(2\text{-Mepy})_8\text{TPyzPz}]^{6+}$ from pH 11 to pH 1.4 upon addition of HCl (*direct* titration) and again to pH 11 by addition of NaOH are shown in Figure 7. Replication of the entire cyclic process shows nearly identical spectral sequences. Figure 8 shows the spectral changes observed in the region 420−800 for the *direct* titration in the pH range 11−4 (a reverse change is produced by moving the pH back to 11). Clean isosbestic points are seen at 458, 602, and 692 nm. When the low pH limit was 1.4, the trends observed remained essentially unchanged, although with some loss of isosbestic points. Noteworthy, this spectral behavior is substantially unaffected in solutions of different ionic strength (2 or 0.2 M NaCl) *or by substitution of the I^- counterion with Cl^-*.

From Figure 7, it is immediately evident that the spectral absorbances in the *direct* and *reverse* processes do not overlap. This is clearly not in line with expectation for processes involving exclusively sequential fast proton-transfer equilibria. Rather, the occurrence of slow steps in

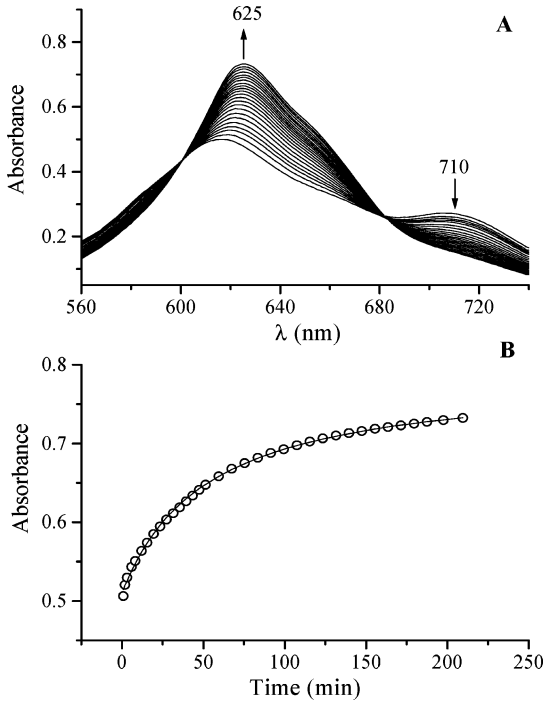

Figure 9. (A) Spectral changes of an aqueous buffered solution (0.01 M $Na_3PO_4 \cdot 12H_2O$, 2.0 M NaCl) of the aggregated $[Mepy_8TPyzPz]^{6+}$ at pH 6.58 as a function of time; isosbestic points are observed at 600 and 683 nm. (B) Absorbance at 625 nm vs time (○) at pH 6.58 and second-order fit (—, $k_{II} = 100\ s^{-1}\ M^{-1}$).

the overall process needs to be considered. This is believed to be related to the existence of different forms of aggregation for the deprotonated species $[(2\text{-Mepy})_8TPyzPz]^{6+}$ and its protonated analogue $[(2\text{-Mepy})_8TPyzPzH_2]^{8+}$.

The above findings are in agreement with the data from stopped-flow experiments (see the Experimental Section for details). In each of these experiments it is seen that the spectrum recorded immediately after mixing does not show appreciable changes from that measured at pH 11.0 down to a value just above pH 2.0, as shown by the normalized 625 nm zero-time absorbances given in Figure 7. This indicates that the deprotonated aggregate species $[(2\text{-Mepy})_8TPyzPz]^{6+}$ present at pH 11 is not undergoing extensive fast protonation in the pH range 11−2 and is also retaining its aggregate structure.

It is also interesting to observe that the zero-time spectrum at each pH value < 11 is not stable, thus signifying that a slow reaction is taking place. In Figure 7, the infinite-time (equilibrium) absorbances ($\lambda = 625$ nm) within the pH range explored are reported. Figure 9A exemplifies the spectral changes which occur for a pH = 6.58 solution of the macrocycle together with the second-order fit (Figure 9B) for the 625 nm absorption vs time. All experiments carried out within the pH range of 9−0.1 gave excellent second-order absorbance vs time plots. The second-order rate constants were found to be strongly dependent on the hydrogen ion concentration as clearly shown in Figure 10 (see later discussion). Despite an intrinsically lower accuracy, it is evident that the plot of the infinite time absorbance (Figure 7) follows the same pattern as the absorbance vs pH curve for the *reverse* titration.

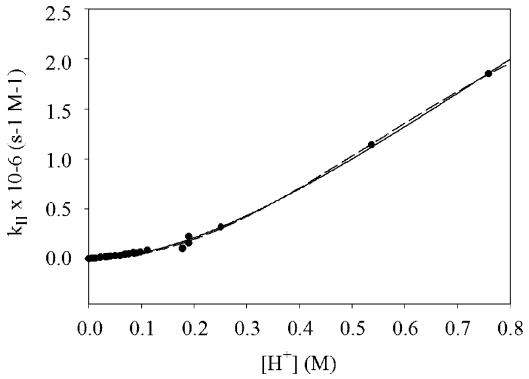

Figure 10. Second-order rate constants vs $[H^+]$ (●) and fit of eq 5 to the experimental values. Best fits are obtained with $m = 1$, $q = 2$, $p = 0$ (solid line) and with $m = 2$, $q = p = 1$ (dashed line).

Full rationalization of the above complex reaction picture is far from being achieved for the following reasons: (a) the macrocycle has different potential protonation sites; (b) the pH values and hence titration data are of uncertain meaning at high proton concentrations; and (c) the exact nature of the aggregate species which exist in the different pH ranges is not known. Nevertheless, avoiding speculation, a few points appear to be sufficiently clear.

For the sake of simplicity let us indicate as B the aggregate of $[(2\text{-Mepy})_8TPyzPz]^{6+}$ stable at pH 11. The zero-time spectra collected with stopped flow experiments reflect a fast protonation reaction as in eq 1

$$B + mH^+ \rightleftharpoons BH_m \text{ (fast)} \tag{1}$$

(charges omitted for simplicity), with

$$[B] = C/(1 + K[H^+]^m) \tag{2}$$

and

$$[BH_m] = CK[H^+]^m/(1 + K[H^+]^m) \tag{3}$$

where $C = [B] + [BH_m]$ and K is the equilibrium constant of reaction 1.

Since only below pH 2.0 are instantaneous spectral modifications detected, the concentration of the protonated BH_m species formed must be very low above this limit as a consequence of BH_m being a very strong acid. The slow second-order reaction that takes place at any given pH suggests a "dimerization" step for B, possibly involving protons in its stoichiometric balance (eq 4).

$$2B + nH^+ \rightarrow B_2H_n \text{ (slow)} \tag{4}$$

The rate equation of reaction 4 can be put into the general form $-(dC/dt) = k[B]^p\,[BH_m]^q$, with $p + q = 2$, and the use of eqs 2 and 3 yields the second-order kinetic equation

$$-(dC/dt) = k_{II}C^2 \tag{5}$$

with

$$k_{II} = kK^q[H^+]^{m\cdot q}/(1 + K[H^+]^m)^2 \tag{6}$$

Table 4. Least-Squares Fit Parameters for Eq 6[a]

m	*q*	*p*	K/M^{-m}	$k/s^{-1}M^{-1}$
1	2	0	0.566	2.06×10^7
2	1	1	0.454	1.12×10^7

[a] The meaning of the "*m*", "*q*", and "*p*" symbols is explained in the text.

The case where $q = 0$ is ruled out since it leads to rate constants which decrease with increasing $[H^+]$. The remaining alternatives ($q = 1$ and 2) both lead to excellent least-squares fits to the experimental points (see curves in Figure 10) with $m = 2$ and 1, respectively. Also the least squares values for both the equilibrium constant *K* and the kinetic constant *k* are not very different as summarized in Table 4.

It can be seen that the order of magnitude of *K* is that which is expected to account for the low pH value required to generate detectable amounts of the protonated form of the macrocycle. All other sets of values for *m*, *p*, and *q* are totally inconsistent with the experiments.

Since, at the same pH, the spectrum measured during the *reverse* titration and that measured at the end of the slow second-order step are virtually the same, it would seem obvious to assign them to the same equilibrium system. However, this is not compatible with the reaction taking place along the *reverse* titration being a mere proton transfer (hence fast) equilibrium since, in such a case, reverting the pH to acidic values from 11 would cause the system to go back through the same equilibrium state sequence.

However, it can be observed that, if the final product of the slow step is a protonated "dimeric" form of the aggregated cation $[(2\text{-Mepy})_8\text{TPyzPz}]^{6+}$ present at pH 11, as suggested by the kinetic results discussed above, the reaction corresponding to the *reverse* titration pattern cannot be a simple deprotonation reaction but must imply, in addition to a reversible proton transfer, the change of the protonated "dimeric" structure to the aggregated cation $[(2\text{-Mepy})_8\text{TPyzPz}]^{6+}$.

Conclusions

A new water-soluble octacationic pyrazinoporphyrazine macrocycle, tetrakis-2,3-[5,6-di{2-(*N*-methyl)pyridiniumyl}-pyrazino]porphyrazine isolated as a hydrated iodide salt, i.e., $[(2\text{-Mepy})_8\text{TPyzPzH}_2](I_8)\cdot 8H_2O$, has been prepared, and its solid state and solution behavior has been examined in detail. Water solution studies indicate that the macrocycle $[(2\text{-Mepy})_8\text{TPyzPzH}_2]^{8+}$ and its corresponding centrally deprotonated cation $[(2\text{-Mepy})_8\text{TPyzPz}]^{6+}$ can exist in the aqueous medium as aggregated species, but the octacation is monomeric under strongly acidic conditions whereas its deprotonated hexacation undergoes disaggregation in pyridine−water mixtures, in neat pyridine, and in several nonaqueous solvents (DMSO, DMF, CH_3CN, C_6H_5CN, CH_3OH). Titration experiments in water solutions indicate a strong tendency of $[(2\text{-Mepy})_8\text{TPyzPzH}_2]^{8+}$ to exist as a deprotonated cation, $[(2\text{-Mepy})_8\text{TPyzPz}]^{6+}$, from pH 11 down to pH 2, which is consistent with the above octacationic unit being a strong acid, most likely stronger than its corresponding unquaternized species $[\text{Py}_8\text{TPyzPzH}_2]$. This behavior can be the result of the incremented electron-deficient properties of the macrocycle when it is quaternized at the pyridine N atoms. Further supporting information on this point is given by UV−visible and electrochemical data on a series of related octacationic macrocycles $[(2\text{-Mepy})_8\text{TPyzPzM}]^{8+}$ (M = $Mg^{II}(H_2O)$, Co^{II}, Cu^{II}, Zn^{II}; $x = 2-5$) described in the following paper.[7] It is important here to point out that the investigated octacation $[(2\text{-Mepy})_8\text{TPyzPzH}_2]^{8+}$ has an acidity strength much higher than that of a related monomeric octacation $[(4\text{-Mepy})_8\text{PzH}_2]^{8+}$, since for the corresponding deprotonated cation $[(4\text{-Mepy})_8\text{Pz}]^{6+}$ protonation starts, under comparable experimental conditions, at pH values > 6, no matter what the ionic strength (NaCl 2.0 or 0.1 M).[6] Most interestingly, therefore, it can be concluded that the currently investigated macrocyclic aggregate has a pK_a value some orders of magnitude lower than that for the monomeric analogue $[(4\text{-Mepy})_8\text{PzH}_2]^{8+}$, thus challenging an earlier claim[6] that this latter species was the strongest acid known in the area of tetrapyrrolic macrocycles.

Acknowledgment. Financial support by the University of Rome La Sapienza and the MIUR (Cofin 2003038084) and the Robert A. Welch Foundation (K.M.K., Grant E-680) is gratefully acknowledged. M.P.D. thanks the Department of Chemistry, University of Houston, for kind hospitality. Thanks are expressed to Prof. P. A. Stuzhin (Ivanovo State University of Chemical Technology, Ivanovo, Russia) and to Dr. Paola Galli for suggestions and useful discussions and to F. Scannerini and M. Manni for experimental help.

Supporting Information Available: An X-ray crystallographic file in CIF format of compounds **1** and **2**, experimental details of X-ray diffraction studies, ORTEP views (Figures S1 and S2), and a table of relevant conformation parameters for compounds **1** and **2** (Table S1). This material is available free of charge via the Internet at http://pubs.acs.org.

IC051084L